



Published in final edited form as:

*J Orthop Res.* 2016 August ; 34(8): 1431–1438. doi:10.1002/jor.23325.

## Longitudinal Changes in the Structure and Inflammatory Response of the Intervertebral Disc Due to Stab Injury in a Murine Organ Culture Model

Adam C. Abraham<sup>1</sup>, Jennifer W. Liu<sup>2</sup>, and Simon Y. Tang<sup>1,2,3</sup>

<sup>1</sup>Department of Orthopedic Surgery, Washington University in St. Louis, 660 S. Euclid, Campus Box 8233, St. Louis 63103, Missouri

<sup>2</sup>Department of Biomedical Engineering, Washington University in St. Louis, One Brookings Drive, Whitaker Hall, Campus Box 1097, St. Louis 63130, Missouri

<sup>3</sup>Department of Mechanical Engineering and Materials Science, Washington University in St. Louis, St. Louis, Missouri

### Abstract

Despite the significant public health impact of intervertebral disc (IVD) degeneration and low back pain, it remains challenging to investigate the multifactorial molecular mechanisms that drive the degenerative cascade. Organ culture model systems offer the advantage of allowing cells to live and interact with their native extracellular matrix, while simultaneously reducing the amount of biological variation and complexity present at the organismal level. Murine organ cultures in particular also allow the use of widely available genetically modified animals with molecular level reporters that would reveal insights on the degenerative cascade. Here, we utilize an organ culture system of murine lumbar functional spinal units where we are able to maintain the cellular, metabolic, and structural, and mechanical stability of the whole organ over a 21-day period. Furthermore, we describe a novel approach in organ culture by using tissues from animals with an NF- $\kappa$ B-luc reporter in combination with a mechanical injury model, and are able to show that proinflammatory factors and cytokines such as NF- $\kappa$ B and IL-6 produced by IVD cells can be monitored longitudinally during culture in a stab injury model. Taken together, we utilize a murine organ culture system that maintains the cellular and tissue level behavior of the intervertebral disc and apply it to transgenic animals that allow the monitoring of the inflammatory profile of IVDs. This approach could provide important insights on the molecular and metabolic mediators that regulate the homeostasis of the IVD.

### Keywords

intervertebral disc degeneration; organ culture; functional spine unit; NF- $\kappa$ B; IL-6

---

Correspondence to: Simon Y. Tang (T: (314) 286-2664; F: (314) 362-0334; TangS@wudosis.wustl.edu). Adam C. Abraham and Jennifer W. Liu contributed equally to this work.

#### AUTHORS' CONTRIBUTIONS

ACA, JWL, and SYT conceived and designed the experiments. ACA and JWL conducted the experiments. ACA, JWL, and SYT analyzed the data and wrote the manuscript.

Lower back pain (LBP) is a highly prevalent and debilitating disease. A recent analysis of the Global Burden of Disease 2010 study<sup>1</sup> identified LBP as the leading cause of disability, affecting 9.4% of the entire population.<sup>2</sup> Alarming, this number appears to be growing at a rate faster than can be accounted for by population increases alone.<sup>2</sup> Clearly, there is an urgent need to understand the disease mechanisms of LBP to develop effective treatment and prevention strategies.

Unfortunately, the etiology of LBP is complex with an array of risk factors among which intervertebral disc (IVD) degeneration ranks one of the highest.<sup>3,4</sup> As the IVD undergoes aging and degeneration, a number of changes occur that affect the IVDs' structural, mechanical, and inflammatory behavior.<sup>5,6</sup> Initially, IVD cellular behavior disrupts the remodeling balance of extracellular matrix (ECM).<sup>6</sup> As this condition progresses, structural degeneration becomes apparent with a progressive loss of glycosaminoglycans (GAGs) within the nucleus pulposus and structural disruption of the annulus fibrosus.<sup>7-9</sup> Mechanical function is gradually reduced and disc height begins to decrease.<sup>10</sup> These changes are often concomitant with the expression of cytokines that exacerbate an inflammatory response which may subsequently promote neutrophil and dorsal root ganglion invasion into the joint space that culminate into development of LBP.<sup>5</sup>

Observing the initiating mechanisms are difficult and costly in humans, particularly when there are many factors contribute to IVD degeneration and eventual LBP. In a laboratory setting however, the organ culture approach enables mechanistic modulation of homeostatic variables by reducing the experimental system to only the native cell population and their surrounding ECM and tissue structure. Such systems make it easier to interpret the direct effects of external stimuli, how they may lead to IVD degeneration, and their ultimate functional and mechanical consequences. Previous efforts in IVD organ culture provided general guidelines regarding limiting tissue swelling and media conditions.<sup>11-14</sup> While large animal models better mimic the biomechanical properties of human IVDs,<sup>15</sup> murine models provide an opportunity to rapidly achieve IVD homeostasis, apply experimental stressors, and leverage the use of the well-established assays and genetically engineered animals to better understand the mechanisms that drive degeneration. We present here a murine organ culture system where the cellular stability and IVD mechanical performance is maintained over culture for 21 days, with particular attention given to the cellular, mechanical, structural, and inflammatory behavior. Using this system, we monitor the functional changes at the cell and tissue level in the IVD in a stab induced injury model to investigate the mechanisms driving disc degeneration.

## METHODS

### Animals and Sample Preparation

All animal experiments were performed with approval from the Washington University Animal Studies Committee. Two strains of mice were used for this study, BALB/c ( $n=16$  Taconic Model #BALB-M, BALB/cAnNTac) and a nuclear factor kappa-B-luciferase reporter animal (NF- $\kappa$ B-luc) which is bred on a BALB/c background ( $n=16$ , Taconic Model #10499, BALB/c-Tg(Reluc)31Xen). The NF- $\kappa$ B-luciferase reporter animals were used for the molecular inflammation experiments to track NF- $\kappa$ B expression longitudinally

throughout the experiment. Animals were euthanized with CO<sub>2</sub> overdose at a flow rate of 2.5–3 L/min for 5 min, allowed 2 min of dwelling time, and then bathed in 70% ethanol for 2 min before dissection. A longitudinal vertical cut was made using a no. 11 blade scalpel on the dorsal surface of the mouse to expose the body cavity. The lumbar spine from each animal was dissected out and excessive soft tissues surrounding the spinal column were removed. Spinal columns were then further dissected into vertebrae-disc-vertebrae functional spinal units (FSUs) at the L1/L2, L3/L4, and L5/L6 discs (Fig. 1A). FSUs were used as opposed to isolated IVDs to reduce swelling and to maintain both the bony and cartilage endplates which have been shown to be critical for nutrient diffusion into the IVD and function.<sup>16</sup> FSUs were rinsed in Hanks buffered salt solution supplemented with 1% penicillin-streptomycin and then randomly assigned to four groups: Control FSUs (Control), stab-injury FSUs (Stab), flash frozen FSUs (Dead), and fresh non-cultured FSUs (Fresh).

### Organ Culture Conditions

Fresh samples were dissected and stored immediately in –80°C, and dead samples were flash frozen in liquid nitrogen. Control, Stab, and Dead FSU samples were cultured for 21 days in 24-well culture plates with each well containing 2 ml of 1:1 Dulbecco's modified Eagle's medium: Nutrient Mixture F-12 (DMEM:F12, Gibco, Carlsbad, CA) supplemented with 20%<sup>12</sup> fetal bovine serum (FBS) and 1% penicillin-streptomycin. All samples were incubated in a sterile incubator that maintained 37°C, 5% CO<sub>2</sub>, 20% O<sub>2</sub>, and >90% humidity.

After an initial culture period of 24 h, the Stab samples were punctured transversely through the anterior side of the IVD using a sterile 27G needle as shown in Figure 1A to induce degeneration. The IVD was carefully aligned in the axial position and then punctured with the needle to a marked depth of 0.5 mm under a dissection microscope. The depth of the puncture was guided by a mark made on the needle at the 0.5 mm length, and the injury was also verified via histology following culture. This puncture injury method causes a complete annular tear and a partial puncture of the nucleus pulposus. This injury method was chosen because previous studies have found that full annular rupture produced through needle puncture rapidly produce a severe degree of degeneration.<sup>17–28</sup> We have confirmed that the complete annular puncture injury model is highly repeatable. Following annular injury by needle puncture, the Stab samples and all other samples were then placed in new plates with fresh media. The media was changed every 48 h to remove waste and replenish nutrients until the end of culture (Fig. 1B).

### Diffusion by Conjugated Fluorescein

A separate set of Dead samples was used to determine whether large molecules and nutrients would diffuse into the IVDs. The FSUs were incubated for 24 h with bovine serum albumin conjugated fluorescein (66 kDa). The samples were then rinsed in Hank's balanced salt solution for 20 s to remove excess reagent and processed for cryo-sectioning. Histological sections were then imaged using a fluorescence microscope (IX-51; Olympus) using fluorescein isothiocyanate (FITC) filtering with 495 nm excitation and 520 nm emission wavelengths. Fluorescence was normalized to unlabeled FSUs to account for tissue auto-fluorescence.

### Viability and Metabolism

Sample viability was tracked longitudinally using the alamarBlue metabolic activity assay (Life Technologies, Carlsbad, CA). Two hundred  $\mu\text{L}$  of reagent was added to each well and incubated for 4 h. Samples were then removed and placed in new plates and the media from the old plate was collected and read using a spectrophotometer (Spectramax M2; Molecular Devices, Sunnyvale, CA) using an excitation frequency of 570 nm and an emission frequency of 585 nm. To verify that IVD-specific cells were viable at the terminal time point, the samples were incubated with tetrazolium nitro blue (0.75 mg/ml, Sigma–Aldrich, St. Louis, MO) for 24 h on the final day of culture and a subset processed for histology sectioning (Histology Section). The nitro blue staining was co-localized with DAPI using a custom MATLAB script, normalized by cross-sectional area, and converted into a viability percentage relative to the Fresh samples.

### Biomechanics by Dynamic Compression

The mechanical behavior of the intact intervertebral discs was determined using strain-controlled dynamic compression (BioDent; Active Life Scientific, Santa Barbara, CA).<sup>29</sup> Using a dissection microscope, the bony vertebral bodies of the FSU were removed from each sample while keeping the cartilaginous endplates intact and attached to the IVD. The IVDs were then adhered to an aluminum platen using cyanoacrylate. The disc height was calculated by taking an average of three measurements on the longitudinal axis of each disc using a laser micrometer (Keyence, Itasca, IL). Disc height was used to calculate the input strain values. The sample was then placed in a phosphate buffered saline bath, preloaded to 0.02 N, and compressed using a sinusoidal waveform at 1 Hz for 20 cycles at the 1% strain level and 5% strain level.<sup>18</sup> The load and displacement values of the IVD were recorded for the entire duration of the test cycle. The average stiffness was determined from the loading phase of the last cycle, and the loss tangent was obtained from the phase angle between load and displacement data.<sup>18</sup>

### Glycosaminoglycan Content

The GAG content of the IVD was quantified using the dimethylmethylene blue (DMMB) assay. Samples were digested in papain solution overnight at 65°C using a block heater. The digests were centrifuged for 10 min at 10,000g and the supernatant was collected. The samples and a standard curve created from chondroitin sulfate derived from bovine trachea (Sigma–Aldrich, St. Louis, MO) were plated on a 96-well plate and 250  $\mu\text{l}$  of DMMB dye was added to each well. The plate was then read at an absorbance frequency of 525 nm using a spectrophotometer. Additionally, a subset of samples were used to observe GAG distribution in the IVD using Safranin-O/Fast Green staining of histological sections (Histology Section).

### Structural Analysis by Disc Height Ratio

To quantify the changes in IVD structure, the height to width ratio was calculated using the Safranin-O stained histological sections by the following method adapted from Fenty et al.<sup>19</sup> For each disc, a manually defined ROI is drawn around the disc space, and an ellipse fitted around the ROI. The major axis of the ellipse is measured and defined as the width. Twenty

evenly spaced lines perpendicular to the major axis of the ellipse were then drawn and extended beyond the ellipse. The disc height was measured by averaging the height at each perpendicular line, and finally the disc height ratio was calculated by dividing average height by width. This process was repeated three times for each IVD using three different histological slices taken near the central sagittal axis of the IVD.

### **Inflammatory Cytokines: IL-6 and NF- $\kappa$ B**

Culture media from the 1-, 3-, and 21-day time points were collected, aliquoted, and stored at  $-80^{\circ}\text{C}$ . The concentration of interleukin-6 (IL-6) was determined using an enzyme-linked immunosorbent assay (Mouse IL-6 ELISA Ready-Set-Go!; Affymetrix eBioscience, San Diego, CA). The FSUs from NF- $\kappa$ B-luciferase animals were imaged on days 1, 5, 13, and 19 to assess NF- $\kappa$ B expression. Ten  $\mu\text{L}$  of 1 mg/ml luciferin solution (Caliper Life Sciences) was added to each well and incubated for 10 at  $37^{\circ}\text{C}$ , 5%  $\text{CO}_2$ , 20%  $\text{O}_2$ , and  $>90\%$  humidity. Samples were imaged for bioluminescence using an IVIS Imaging System 100 (Xenogen Corp.) using a 10 s exposure time and a bin setting of 2. A photograph image was taken concurrently and overlaid with the bioluminescence image to identify the anatomical location of NF- $\kappa$ B expression in the IVDs. Using Living Image software (PerkinElmer, Waltham, MA) contoured ROIs were drawn around each disc, and NF- $\kappa$ B expression was measured and normalized to area giving units of photons/s/cm<sup>2</sup>/steradian.

### **Histology**

Samples used to determine IVD diffusion (Diffusion Section) were fixed in 10% formalin for 24 h, infiltrated with 30% sucrose for 24 h, and finally embedded and frozen in optimal cutting temperature compound. The samples were then cryo-sectioned using a cryostat and tape transfer system. Samples used to determine GAG content and structure were fixed in 4% paraformaldehyde for 24 h, decalcified in 5% formic acid for 48 h, and embedded in paraffin. The samples were sectioned at 5  $\mu\text{m}$  thickness and then stained using Safranin-O with a Fast Green counterstain.

### **Statistics**

Viability, IL-6 production, and NF- $\kappa$ B luminescence were compared at each time point to their respective controls using a two-way ANOVA with a Sidak's multiple comparisons test. Mechanical, compositional, and structural data were compared using a one-way ANOVA with a Dunnett's multiple comparisons test. Significance was considered to be  $p < 0.05$ . All comparisons are powered to a minimum  $1-\beta$  of 0.6 or higher. All statistical analyses were performed using GraphPad Prism software (Prism 6.0; Graphpad Software Inc., La Jolla, CA).

## **RESULTS**

Incubating the sample with BSA-fluorescein revealed that passive diffusion adequately delivers the molecules throughout the entire IVD, as evidenced by the ubiquitous presence of BSA-fluorescein in both the annulus fibrosus and nucleus pulposus regions of the IVD. Since BSA-fluorescein is a relatively large molecule at 66 kDa, smaller amino acids, critical nutrients, would also undoubtedly be able to passively permeate the IVD (Fig. 2E and F).

The alamarBlue assay confirmed sample throughout the duration of the culture period. The metabolic activity readings of the Control group samples did not vary throughout culture, but were significantly higher than the Dead group samples (Fig. 2A), as expected. Furthermore, IVD-specific cell viability was confirmed with positive staining using nitro blue tetrazolium chloride (Fig. 2B–D). Furthermore, both the Dead and Stab groups showed significantly reduced cellular viability compared to the control (Fig. 2B), while the control group after 21 days of culture remained statistically indistinguishable from the fresh samples (Fig. 2B,  $p=0.242$ ).

IVD mechanical functionality was maintained in culture and was statistically indistinguishable from the Control cultured samples and the Fresh harvested samples across multiple measures (Fig. 3). As expected, the mechanical insult of the Stab group produced a significant reduction in tissue stiffness and viscoelasticity at both the 1% and 5% strain levels. The mechanical performance of the Dead samples degraded over the 21 days in the culture media without the presence of cells to maintain the IVD matrix.

GAG concentration was also not different between Control and Fresh samples (Fig. 4A), however, the GAG concentration of the Stab group was significantly lower. This was confirmed qualitatively from the paraffin histology slices as the Control samples have more positive red staining than the Stab samples (Fig. 4B–D).

At the 24-h time point, both Control and Stab samples had a high concentration of inflammatory cytokines (Fig. 5). After 72 h, IL-6 production was significantly reduced in the Control samples, but maintained at a high level in the Stab samples. Similarly, the NF- $\kappa$ B luminescence readings for the Control samples declined significantly by day 5, while NF- $\kappa$ B luminescence for the Stab group remained elevated throughout the culture period.

At the 24-h time point, both Control and Stab samples had high levels of NF- $\kappa$ B luminescence and expression (Fig. 5). NF- $\kappa$ B luminescence for the Control samples declined significantly by day 5, but it remained elevated throughout the culture period for the Stab samples. Similarly, after the 72-h time point, IL-6 inflammatory cytokine production was significantly reduced in the Control samples, but it was maintained at a high level in the Stab samples.

## DISCUSSION

Combining the successful elements of previous organ culture models,<sup>20,21</sup> we were able to provide another step forward toward an in vitro platform for examining the mechanisms of IVD degeneration. In assessing the viability of our current 21-day organ culture model, we considered IVD nutrient diffusion, cell viability, mechanical properties, structural changes, GAG content, and molecular inflammation, as all of these factors are critical toward the stability and function of the IVD.

Early attempts at maintaining discs in culture found that structural integrity of the entire disc is crucial to maintaining functionality and cell viability. Chiba et al. attempted to retain disc structure in rabbit IVDs by embedding the tissue in alginate gel, reducing free swelling, which improved maintenance.<sup>11</sup> To simplify this approach while also retaining disc

structure, it was determined that the cartilage end plates were required as part of the organ culture system,<sup>22</sup> and we thus chose to culture whole FSUs as opposed to isolated IVDs. In our study, there were no significant changes in IVD morphology, disc height, or signs of swelling following 21-day long-term culture, which we believe is largely due to the maintenance of the bony and cartilage endplates on the FSU. In preliminary experiments, we saw that isolated IVDs in culture vertebrae endplates result in disc height and swelling.

Other groups have also attempted murine organ culture with varying results. Yan et al.<sup>20</sup> and Pelle et al.<sup>21</sup> both cultured isolated IVDs for up to 14 days, whereas in our study, we cultured FSUs which contained intact cartilage endplates and vertebrae for up to 21 days. These two groups also used between 2% and 10% FBS whereas we used 20% FBS. We have shown that IVD organ cultures are able to maintain their native functional phenotype in long-term culture conditions and are responsive to external stimuli, for example, stab, and additionally found that IVDs remained mechanically unchanged following culture.

Another important aspect of maintaining disc health is the selection of media and serum supplementation. In large animals, it became crucial to provide anti-coagulants and aspirate the end-plates in order to keep nutrient channels open and ensure the viability of cells.<sup>16</sup> In small animal models, this has not been a concern as the media diffuse through the annulus and reach the cells inside the nucleus pulposus when the end-plates and even the vertebrae are left intact.<sup>12,23</sup> In our study, we used BSA-fluorescein to quickly confirm these results, and found that relatively large molecule was able to readily diffuse into the intact disc structure. Because there are no significant differences in structure or composition in fresh, dead, and control IVDs, we did not expect differences in passive diffusion, although certainly the cellular metabolism is altered in these groups. It is worth noting that under the presumption that intact disc is less diffusible than the structurally compromised stabbed IVDs, we did not examine the diffusion of the stabbed samples. Future studies that examine nutrient transport over time and under various treatments could be useful, but was not the focus of this present study.

Wide ranges of formulations have been attempted from serum-free approaches up to 20% and various growth factors. However, in agreement with Ponnappan et al.,<sup>12</sup> we found a mix of DMEM:F12 with 20% FBS and 1% penicillin-streptomycin was appropriate for maintaining mouse discs up to 21 days. It is important to remember that our treatment conditions are tailored toward maintaining murine IVDs for long term culture, and may not be optimal for large animal model IVD organ cultures or the maintenance of other cell types. Due to its imprecise composition and lot-to-lot variability, FBS may have undesirable effects on the IVD cells. These effects can be somewhat mitigated with a balanced experimental design as we have done here, by ensuring every treatment receive the same lot and batch of FBS.

An important advantage of using organ culture as opposed to cell culture is that cells retain interactions with their native ECM environment. These interactions are crucial in maintaining cell function and phenotype, and it has been shown that cell dedifferentiation occurs during in vitro monolayer expansion of both annulus fibrosis and nucleus pulposus cells.<sup>24</sup> In this study, annulus fibrosis cells remained elongated and fibroblast-like while

nucleus pulposus remained round and chondrocyte-like throughout the 21-day culture period, as shown in histological analysis. This finding illustrates the importance of the native ECM architecture in maintaining IVD cell phenotype, and also highlights a key advantage of utilizing the organ culture technique over monolayer cell culture.

Additionally, using murine tissues for organ culture allows us to draw upon the extensive number of genetically engineered strains to understand the cellular mechanisms that regulate the degenerative processes within the disc. We demonstrate this possibility through the longitudinal bioluminescence imaging of NF- $\kappa$ B. These results also show that the IVD is capable of responding to environmental stressors by producing proinflammatory cytokines throughout culture. The process of removing the spine and dissecting lumbar FSUs is obviously a major environmental perturbation and stressor. As expected, the cultured IVDs in all treatment groups show very high levels of both NF- $\kappa$ B and IL-6 cytokine production at the 24-h time point that are similar to Fresh group samples. This initial proinflammatory response diminishes in the Control group samples, but remains elevated in the Stab group samples, showing that the organ culture system is capable of dynamically responding to its environment. The enhanced inflammatory response is also likely linked to the observed decrease in GAG content and decreased mechanical properties. Consistent with Rousseau et al., stab and puncture incisions induce a cascade of biological changes such as loss of cellular viability, increased inflammation, and cell apoptosis, all of which are hallmarks of pathological degeneration.<sup>18</sup> Future work is required to examine whether the IVD cells have de-differentiated as a result of these changes.

A caveat of using mice or other small animals is the inability to recapitulate the progressively restrictive diffusion gradients, a well-known facet of human disc pathophysiology.<sup>6,15</sup> One approach is to starve the cells within the disc by reducing media nutrition<sup>25</sup>; however, this is then externally regulated rather than a by-product of the intrinsic degenerative process. When considering this mechanism researchers have leveraged larger animal tissues,<sup>14</sup> however, maintaining healthy discs requires the addition of cyclic loading to aid with nutrient transport and the evacuation of waste.<sup>26,27</sup> Large animal culture models provide valuable insight into nutrient supply, loading regimens that may be beneficial or pathological to the disc, and in some cases the capability to track longitudinal changes in IVD function during the culture.

We demonstrate here the versatility of the murine organ culture system, whereby the cellular, mechanical, and structural stability of the intervertebral disc is maintained throughout culture, as well as leverage the power of genetically modified mice that allows us to monitor the production of the inflammatory cytokines longitudinally during early degeneration.

## Acknowledgments

Grant sponsor: Washington University Musculoskeletal Research Center; Grant number: NIH P30 AR057235; Grant sponsor: Molecular Imaging Center; Grant number: NIH P50 CA094056; Grant sponsor: Metabolic Skeletal Disorders Training Program; Grant number: NIH 5T32AR060719.

We would also like to acknowledge the Washington University Molecular Imaging Core for their assistance in bioluminescence imaging.



## References

1. Murray CJL, Vos T, Lozano R, et al. Disability-adjusted life years (DALYs) for 291 diseases and injuries in 21 regions, 1990–2010: a systematic analysis for the Global Burden of Disease Study 2010. *Lancet*. 2012; 380:2197–2223. [PubMed: 23245608]
2. Hoy D, March L, Brooks P, et al. The global burden of low back pain: estimates from the Global Burden of Disease 2010 study. *Ann Rheum Dis*. 2014; 73:968–974. [PubMed: 24665116]
3. Schwarzer AC, Aprill CN, Derby R, et al. The prevalence and clinical features of internal disc disruption in patients with chronic low back pain. *Spine (Phila Pa 1976)*. 1995; 20:1878–1883. [PubMed: 8560335]
4. Luoma K, Riihimäki H, Luukkonen R, et al. Low back pain in relation to lumbar disc degeneration. *Spine (Phila Pa 1976)*. 2000; 25:487–492. [PubMed: 10707396]
5. Risbud MV, Shapiro IM. Role of cytokines in intervertebral disc degeneration: pain and disc content. *Nat Rev Rheumatol*. 2014; 10:44–56. [PubMed: 24166242]
6. Urban J, Roberts S. Degeneration of the intervertebral disc. *Arthritis Res Ther*. 2003; 5:1–48.
7. Johannessen W, Auerbach JD, Wheaton AJ, et al. Assessment of human disc degeneration and proteoglycan content using T1rho-weighted magnetic resonance imaging. *Spine (Phila Pa 1976)*. 2006; 31:1253–1257. [PubMed: 16688040]
8. Lyons G, Eisenstein SM, Sweet MB. Biochemical changes in intervertebral disc degeneration. *Biochim Biophys Acta*. 1981; 673:443–453. [PubMed: 7225426]
9. Iatridis JC, MacLean JJ, O'Brien M, et al. Measurements of proteoglycan and water content distribution in human lumbar intervertebral discs. *Spine (Phila Pa 1976)*. 2007; 32:1493–1497. [PubMed: 17572617]
10. Iatridis JC, Setton LA, Weidenbaum M, et al. Alterations in the mechanical behavior of the human lumbar nucleus pulposus with degeneration and aging. *J Orthop Res*. 1997; 15:318–322. [PubMed: 9167638]
11. Chiba K, Andersson GB, Masuda K, et al. A new culture system to study the metabolism of the intervertebral disc in vitro. *Spine (Phila Pa 1976)*. 1998; 23:1821–1827. discussion 1828. [PubMed: 9762737]
12. Ponnappan RK, Markova DZ, Antonio PJ, et al. An organ culture system to model early degenerative changes of the intervertebral disc. *Arthritis Res Ther*. 2011; 13:R171. [PubMed: 22018279]
13. Seol D, Choe H, Ramakrishnan PS, et al. Organ culture stability of the intervertebral disc: rat versus rabbit. *J Orthop Res*. 2013; 31:838–846. [PubMed: 23456659]
14. Korecki CL, MacLean JJ, Iatridis JC. Characterization of an in vitro intervertebral disc organ culture system. *Eur Spine J*. 2007; 16:1029–1037. [PubMed: 17629763]
15. Grunhagen T. Nutrient supply and intervertebral disc metabolism. *J Bone Joint Surg Am*. 2006; 88:30. [PubMed: 16595440]
16. Gantenbein B, Grünhagen T, Lee CR, et al. An in vitro organ culturing system for intervertebral disc explants with vertebral endplates: a feasibility study with ovine caudal discs. *Spine (Phila Pa 1976)*. 2006; 31:2665–2673. [PubMed: 17077734]
17. Lai A, Moon A, Purmessur D, et al. Annular puncture with tumor necrosis factor-alpha injection enhances painful behavior with disc degeneration in vivo. *Spine J*. 2016; 16:420–431. [PubMed: 26610672]
18. Iatridis JC, Michalek AJ, Purmessur D, et al. Localized intervertebral disc injury leads to organ level changes in structure, cellularity, and biosynthesis. *Cell Mol Bioeng*. 2009; 2:437–447. [PubMed: 21179399]
19. Fenty M, Crescenzi R, Fry B, et al. Novel imaging of the intervertebral disk and pain. *Global Spine J*. 2013; 3:127–132. [PubMed: 24436863]
20. Yan Z, Yin L, Wang Z, et al. A novel organ culture model of mouse intervertebral disc tissues. *Cells Tissues Organs*. 2016; 201:38–50. [PubMed: 26447649]
21. Pelle DW, Peacock JD, Schmidt CL, et al. Genetic and functional studies of the intervertebral disc: a novel murine intervertebral disc model. *PLoS ONE*. 2014; 9:e112454. [PubMed: 25474689]

22. Lee CR, Iatridis JC, Poveda L, et al. In vitro organ culture of the bovine intervertebral disc: effects of vertebral endplate and potential for mechanobiology studies. *Spine (Phila Pa 1976)*. 2006; 31:515–522. [PubMed: 16508544]
23. Stannard JT, Edamura K, Stoker AM, et al. Development of a whole organ culture model for intervertebral disc disease. *J Orthop Transl*. 2016; 5:1–8.
24. Kluba T, Niemeyer T, Gaissmaier C, et al. Human annulus fibrosis and nucleus pulposus cells of the intervertebral disc: effect of degeneration and culture system on cell phenotype. *Spine (Phila Pa 1976)*. 2005; 30:2743–2748. [PubMed: 16371897]
25. Bibby SRS, Urban JPG. Effect of nutrient deprivation on the viability of intervertebral disc cells. *Eur Spine J*. 2004; 13:695–701. [PubMed: 15048560]
26. Gantenbein B, Illien-Jünger S, Chan SCW, et al. Organ culture bioreactors—platforms to study human intervertebral disc degeneration and regenerative therapy. *Curr Stem Cell Res Ther*. 2015; 10:339–352. [PubMed: 25764196]
27. Korecki CL, MacLean JJ, Iatridis JC. Dynamic compression effects on intervertebral disc mechanics and biology. *Spine (Phila Pa 1976)*. 2008; 33:1403–1409. [PubMed: 18520935]
28. Rousseau M-AA, Ulrich JA, Bass EC, et al. Stab incision for inducing intervertebral disc degeneration in the rat. *Spine (Phila Pa 1976)*. 2007; 32:17–24. [PubMed: 17202887]
29. Liu JW, Abraham AC, Tang SY. The high-throughput phenotyping of the viscoelastic behavior of whole mouse intervertebral discs using a novel method of dynamic mechanical testing. *J Biomech*. 2015; 48:2189–2194. <http://doi.org/10.1016/j.jbiomech.2015.04.040>. [PubMed: 26004435]

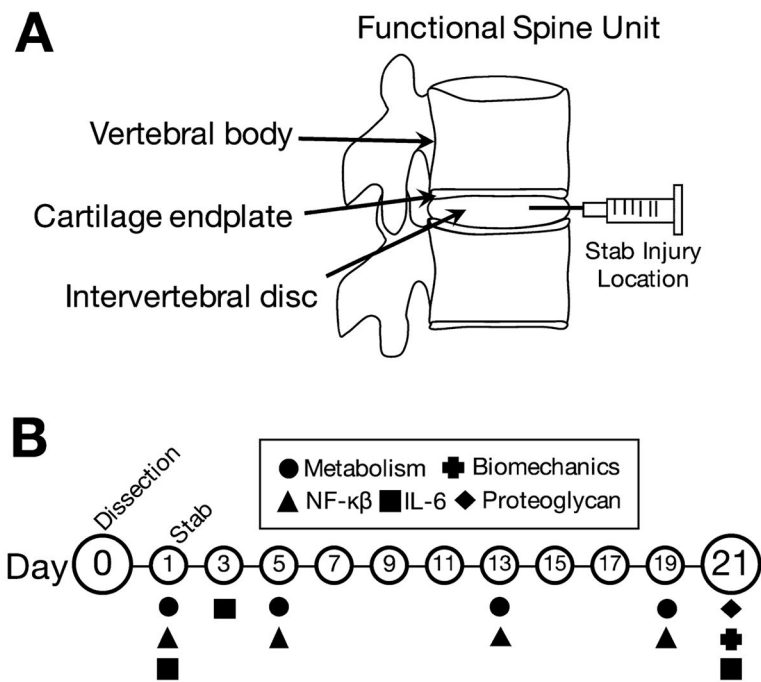


**Figure 1.** Study design. (A) Murine functional spine units consisting of intact vertebral bodies, cartilage endplates, and the intervertebral disc. Stab injury location and direction are indicated with the needle. (B) The samples were maintained for 21 days and assayed longitudinally for metabolic activity and inflammatory behavior, and terminally for GAGs content and biomechanical function.

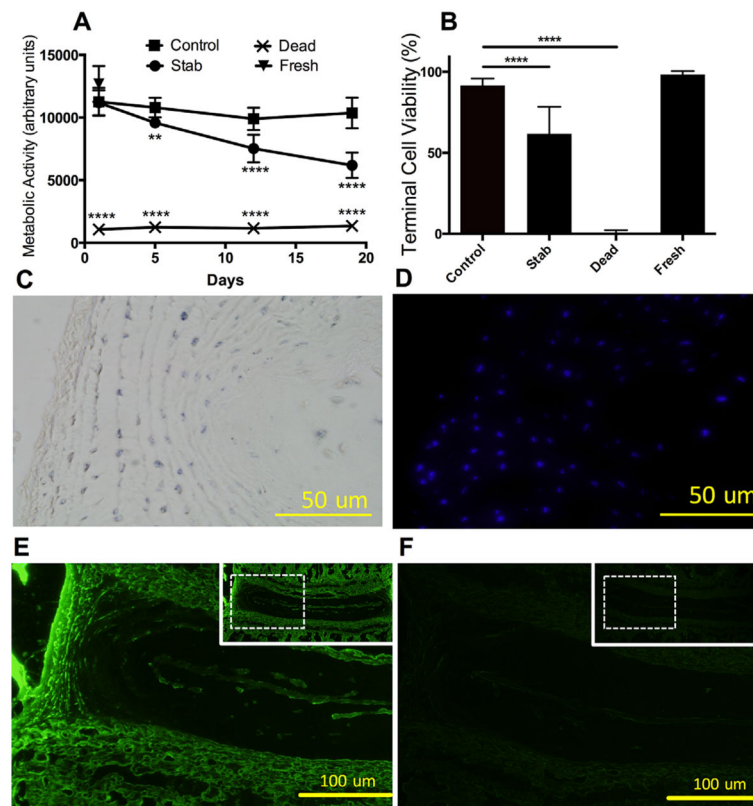


**Figure 2.** Intervertebral disc cell metabolism and viability. (A) Viability of the Fresh, Control, and Stab samples were significantly higher than the flash frozen dead controls at all time points. (B) At the end of the 21-day culture, the IVD cells in all treatment groups except Dead were still viable as evident by nitro blue tetrazolium chloride staining. (C and D) Positive blue staining from nitro blue tetrazolium chloride that co-localized DAPI-labeled cells. (E and F) Positive fluorescein labeled BSA was observed throughout the entire disc space, indicating adequate permeability for nutrients to diffuse through the tissue compared to an unlabeled control. Note: All bars and lines represent mean and standard deviations, and significance is denoted by \*  $p < 0.05$ , \*\*  $p < 0.01$ , \*\*\*  $p < 0.001$ .

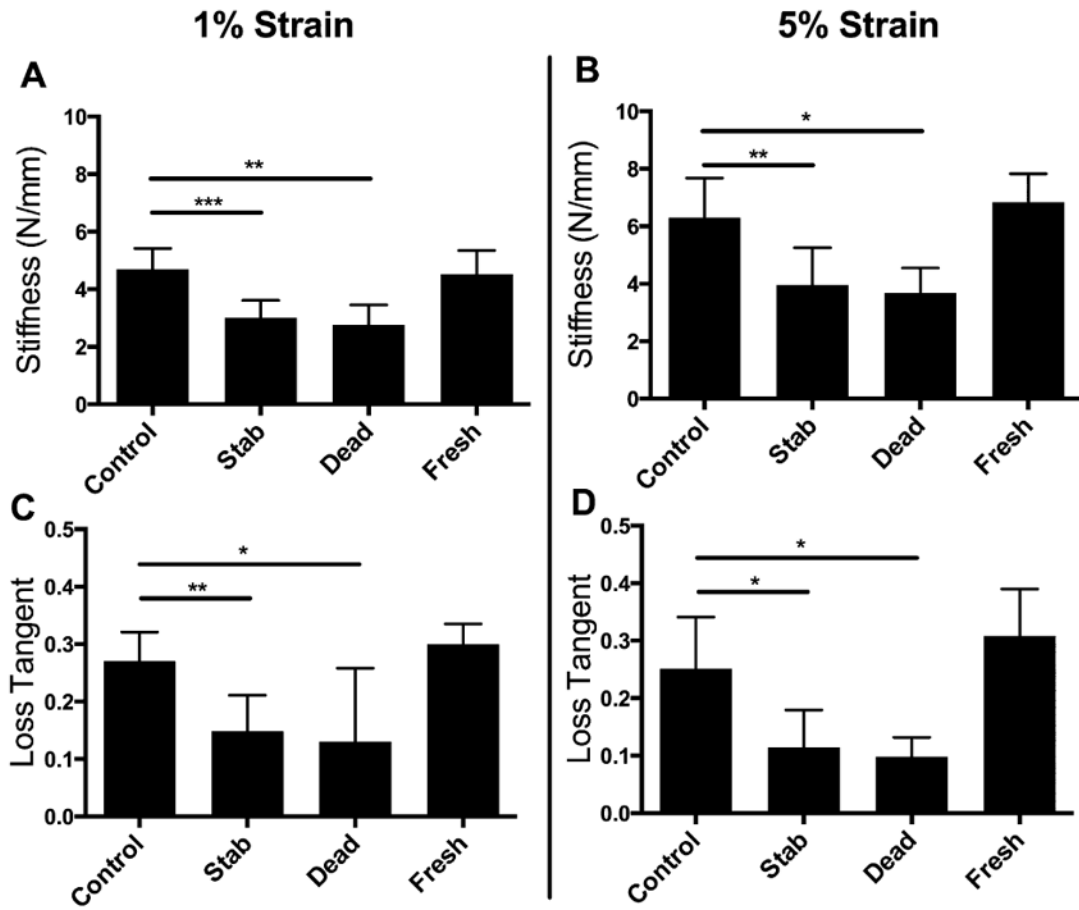


**Figure 3.**

The Control samples were significantly (A and C) stiffer and more (B and D) viscoelastic than either the Stab or Dead samples for both 1% and 5% strain levels. There were no detectable differences between the Control and Fresh group samples in terms of stiffness or viscoelasticity. Note: All bars and lines represent mean and standard deviations, and significance is denoted by \*  $p < 0.05$ , \*\*  $p < 0.01$ , \*\*\*  $p < 0.001$ .

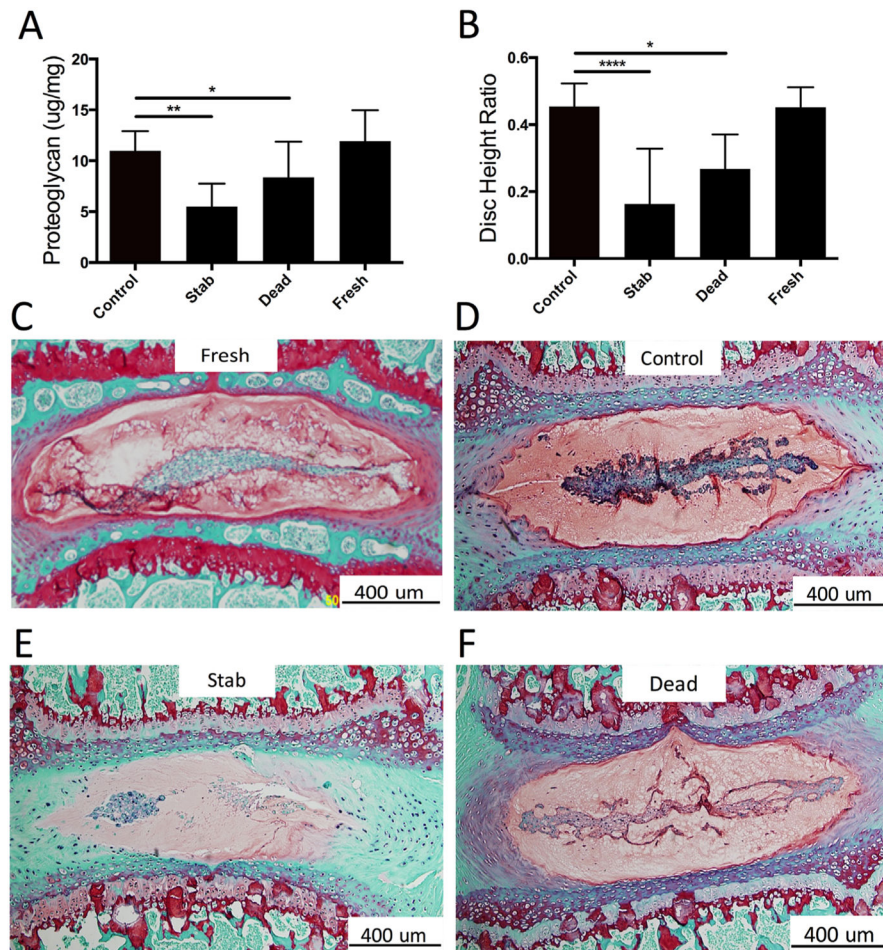


**Figure 4.** Structure and composition of culture IVDs. (A) GAGs was significantly reduced in the Stab and Dead group discs compared to the Controls. (B) Similarly, the disc height ratio was decreased for the Stab and Dead group. (C and D) Positive Safranin-O staining reveals the maintained presence of GAGs in the Control samples relative to the Fresh group samples. (E) The stabbed sample showed a decreased level of Safranin-O staining, indicating loss of GAGs. There is a noticeable loss of the notochordal band in the nucleus pulposus region, presence of cell clustering, and loss of GAGs at the AF-NP interface. (F) The dead samples also appeared to show positive, albeit reduced GAG staining. Note: All bars and lines represent mean and standard deviations, and significance is denoted by \* $p < 0.05$ , \*\* $p < 0.01$ , \*\*\* $p < 0.001$ , \*\*\*\* $p < 0.0001$ .

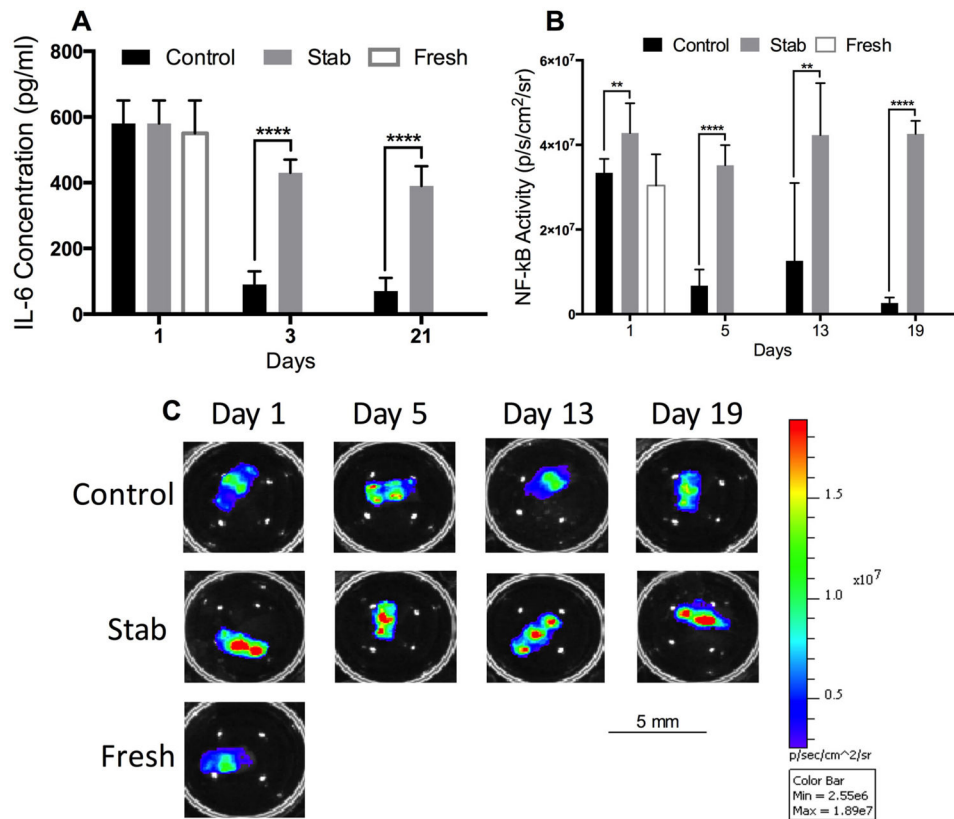


**Figure 5.** Proinflammatory cytokines of cultured IVDs. (A) All treatment groups showed a high level of IL-6 production immediately following removal from the animals. However, by the 3-day time point this was reduced drastically in the Control samples while maintained at high levels in the Stab samples throughout the entire 21-day culture period. (B) Similarly, the NF- $\kappa$  $\beta$  was initially high in the first 24-h period of culture but was significantly less in the Control group by the 5-, 13-, and 19-day time points. (C) Representative of NF- $\kappa$  $\beta$  as measured by bioluminescence for each treatment group at each time point. Note: All bars and lines represent mean and standard deviations, and significance is denoted by \*\*  $p < 0.01$ , \*\*\*  $p < 0.001$ , \*\*\*\*  $p < 0.0001$ .